



HAL
open science

Wearable wireless biosensors for spatiotemporal grip force profiling in real time

Rongrong Liu, Florent Nageotte, Philippe Zanne, Michel de Mathelin, Birgitta Dresp

► **To cite this version:**

Rongrong Liu, Florent Nageotte, Philippe Zanne, Michel de Mathelin, Birgitta Dresp. Wearable wireless biosensors for spatiotemporal grip force profiling in real time. 7th E-Conference on Sensors and Applications ECSA2020, Nov 2020, Zürich (Webinar), Switzerland. hal-03009559

HAL Id: hal-03009559

<https://hal.science/hal-03009559>

Submitted on 17 Nov 2020

HAL is a multi-disciplinary open access archive for the deposit and dissemination of scientific research documents, whether they are published or not. The documents may come from teaching and research institutions in France or abroad, or from public or private research centers.

L'archive ouverte pluridisciplinaire **HAL**, est destinée au dépôt et à la diffusion de documents scientifiques de niveau recherche, publiés ou non, émanant des établissements d'enseignement et de recherche français ou étrangers, des laboratoires publics ou privés.

Wearable wireless biosensors for spatiotemporal grip force profiling in real time

Rongrong Liu¹, Florent Nageotte¹, Philippe Zanne¹, Michel de Mathelin¹ and Birgitta Dresplangley^{2,*}

¹ ICube Lab Robotics Department Strasbourg University UMR 7357 CNRS; rongrong.liu@unistra.fr; Nageotte@unistra.fr; zanne.philippe@unistra.fr; demathelin@unistra.fr;

² ICube Lab UMR 7357 Centre National de la Recherche Scientifique CNRS; birgitta.dresp@unistra.fr;

* Correspondence: birgitta.dresp@unistra.fr;

Full paper Presented at the 7th Electronic Conference on Sensors and Applications, 15 – 30 November 2020;

Available online: <https://ecsa-7.sciforum.net/>.

Abstract: The temporal evolution of individual grip force profiles of a novice using a robotic system for minimally invasive endoscopic surgery is analyzed on the basis of thousands of individual sensor data recorded in real time through a wearable wireless sensor glove system. The spatio-temporal grip force profiles from specific sensor locations in the dominant hand performing a four-step pick-and-drop simulator task reveal skill-relevant differences in force deployment by the small finger (fine grip force control) and the middle finger (gross grip force contribution) by comparison with the profiles of a highly proficient expert. Cross-disciplinary insight from systems neuroscience, cognitive behavioral science, and robotics, with implications for biologically inspired AI for human-robot interaction, highlight the functional significance of spatio-temporal grip force profiling.

Keywords: wearable sensor technology; human grip force; functional analysis; image guided surgical training; simulator task; robot assistance; spatio-temporal skill profiling; human-robot interaction; real time

1. Introduction

Wearable wireless sensor systems are currently developed for the monitoring of health data, exercise activities, and other performance data. Unlike conventional approaches, such devices enable the convenient, continuous, and unobtrusive monitoring of a user's behavioral signals in real time. In previous work [1,2], we have used a wireless sensor glove system for human-robot interaction within a system prototype designed for minimally invasive endoscopic surgery. Functionally motivated analyses of thousands of human grip force data, collected from various sensor locations in the dominant and non-dominant hands of experts, trainees, and novice surgeons in image-guided task simulations, have shown specific differences between the grip force profiles of individual users as a function of task skill level and expertise in using the robotic system. Experts and non-experts employ different grip-force strategies reflected by differences in total amount of grip force deployed by the same fingers of the same hand. Here in this work, we show further functional analyses of thousands of individual grip force data leading the way towards task-specific grip force monitoring in real time, as clarified in the discussion

further below. Task specific sensor data from a complete novice and a highly proficient expert user are exploited here in terms of spatio-temporal variations in average grip force, computed on the basis of data recorded from three task-relevant sensor locations in the dominant hand: 1) the middle phalanx of the middle finger, which mostly contributes to gross force deployment [3,4,5], necessary for lifting weighty objects but useless for skillful execution of the robotic precision task here, 2) the middle phalanx of the small finger, which allows for fine grip force control [3,4,5,6], critically important in subtle precision grip tasks like the one studied here, and 3) the middle phalanx of the ring finger, which is among the least important in grip force control across a variety of tasks and weights lifted, as discussed previously [3,4,5,6]. The spatio-temporal grip force profiles of the novice and the expert are compared across ten successive task sessions for repeated execution of the pick-and-drop robotic simulator task with four critical steps:

1. Activate and move tool towards object location; requires movement ahead in depth along a virtual z-axis in 2D image plane
2. Open and close tool-tip grippers to grasp and lift object
3. Move tool with object to target location; requires lateral movement along x-axis of 2D image plane
4. Open tool-tip grippers to drop object in box.

To accomplish these steps in minimal task time and with maximal precision (i.e. no tool trajectory corrections, no incidents) requires skillful manipulation of the task-relevant (left or right) handle of the robotic system (see Materials and Methods). The novice's dominant hand is the right hand, the expert's dominant hand is the left hand.

2. Materials and Methods

The robotic system is designed for bi-manual endoscopic surgical interventions; the simulator task from this study here solicits only one, in the present case the dominant hand.

2.1 Slave Robotic System

The slave robotic system is built on the Anubis® platform of Karl Storz and consists of three flexible, cable-driven sub-systems for robot-assisted endoscopic surgery, described in detail in our previous work [1] available at: <https://www.mdpi.com/1424-8220/19/20/4575/htm>.

2.2 Master/Slave Control

The slave robot is controlled at the joint level by a position loop running at 1000 Hz on a central controller. The master side consists of two specially designed interfaces, which are passive mobile mechanical systems. Each of the two handles has 3 DoF, which translate for controlling instrument insertion, rotate around a horizontal axis for controlling instrument rotation, and rotate around a final axis (moving with the previous DoF) for controlling instrument bending. Each handle is also equipped with a trigger and with a small four-way joystick for controlling additional DoF. In the experiments here, the trigger is operated with the index finger of a given hand for controlling grasper opening and closing.

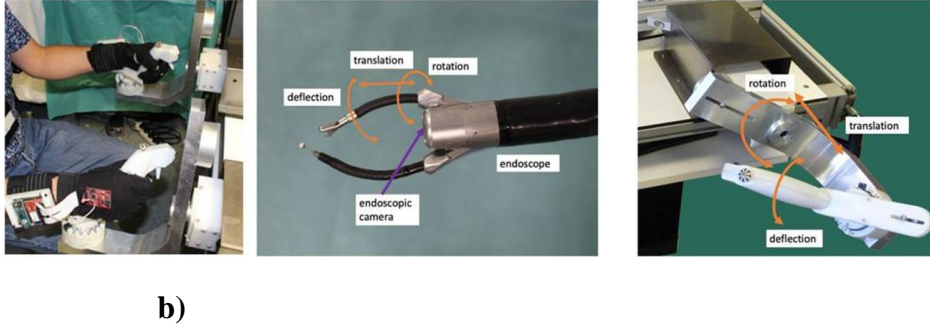


Figure 1. Expert wearing the sensor gloves while manipulating the robotic master/slave system - **a)**. Direction and type of tool-tip and control movements - **b)**.

A high-level controller running in real-time Linux OS communicates with the master interfaces and provides reference positions to the slave central controller. The user sits in front of the master console and looks at the endoscopic camera view displayed on the screen in front of him/her at a distance of about 80 cm while holding the two master handles, which are about 50 cm away from each other. Seat and screen heights are adjustable to optimal individual comfort. The two master interfaces are identical and the two slave instruments they control are also identical. Therefore, for a given task the same movements need to be produced, whatever hand the user is instructed to use (left or right). The master interfaces are statically balanced and all joints exhibit low friction; therefore, only minimal forces are required to produce significant movement in any direction. A snapshot view of a user wearing the sensor gloves while manipulating the system is shown in Figure 1a; Figure 1b shows directions and types of tool-tip and control movements.

2.3 Sensor glove design

The robotic system having its own grip style design, a specific wearable sensor glove system with inbuilt Force Sensitive Resistors (FSR) was developed, one for each hand.

2.3.1 Hardware

The gloves designed for the study each contain twelve FSR, in contact with twelve specific locations on the inner surface of the hand [1,2], including those three for which data are shown here. Two layers of cloth were used and the FSR were inserted between the layers. The FSR were sewn to the cloth around the conducting surfaces (active areas) and did not interact, neither directly with the skin of the subject, nor with the master handles, which provided a comfortable feel when manipulating the system. FSR with a needle and thread. The electrical connections of the sensors are individually routed to the dorsal side of the hand and brought to a soft ribbon cable, connected to a small and very light electrical casing, strapped onto the upper part of the forearm and equipped with an Arduino microcontroller. Each FSR was soldered to 10K Ω pull-down resistors to create a voltage divider, and the voltage read by the analog input of the Arduino is given by (1)

$$V_{out} = RPDV_{3.3}/(RPD+R_{FSR}) \quad (1)$$

where R_{PD} is the resistance of the pull down resistor, R_{FSR} is the FSR resistance, and $V_{3.3}$ is the 3.3 V supply voltage. FSR resistances can vary from 250Ω when subject to 20 Newton (N) to more than $10M\Omega$ when no force is applied at all. The generated voltage varies monotonically between 0 and 3.22 Volt, as a function of the force applied, which is assumed uniform on the sensor surface. In the experiments here, forces applied did not exceed 10N, and voltages varied within the range of [0; 1500] mV. The relation between force and voltage is almost linear within this range. It was ensured that all sensors have similar calibration curves. Thus, all following comparisons are directly between voltage levels at the millivolt (mV) scale. Regulated 3.3V is provided to the sensors from the Arduino, and power is provided by a 4.2V Li-Po battery enabling wireless use of the glove system. The battery voltage level is controlled during the whole duration of the experiments by the Arduino, and displayed continuously on the user interface. The glove system is connected to a computer for data storage via Bluetooth-enabled wireless communication running 115200 bits-per-second (bps).

2.3.2 Software

The software of the glove system is divided into two parts: one running on the gloves, and one running on the computer algorithm for data collection. Each of the two gloves is sending data to the computer separately, and the software reads the input values and stores them on the computer according to header values indicating their origin. The software running on the Arduino is designed to acquire analog voltages provided by the FSR every 20 milliseconds (msec) at a 50 Hz rate. In every loop, input voltages are merged with their time stamps and sensor identification. This data package is sent to the computer via Bluetooth.

3. Results

The raw data from three (see Table 1) of the twelve sensor locations in the dominant hands of the novice and the expert were analyzed.

Table 1: Task-relevant sensor locations (dominant hand) from which the spatio-temporal grip force profiles shown here were drawn

<i>Sensor</i>	<i>Finger</i>	<i>Anatomical reference</i>
S5	Middle	Middle Phalanx
S6	Ring	Middle Phalanx
S7	Pinky	Middle Phalanx

Individual temporal grip force profiles were plotted in terms of average peak amplitudes (AmV) for fixed successive temporal windows of 2000 msec in a given individual session. With one signal per 20 msec and 100 signals per time window of 2000 msec, we have $AmV = mV_{total}/100$,

which is the total sum of mV recorded in the time window given divided by the total number of signals in the time window. Figure 2 shows these profiles for the first and the last individual sessions for sensors 5, 6, and 7.

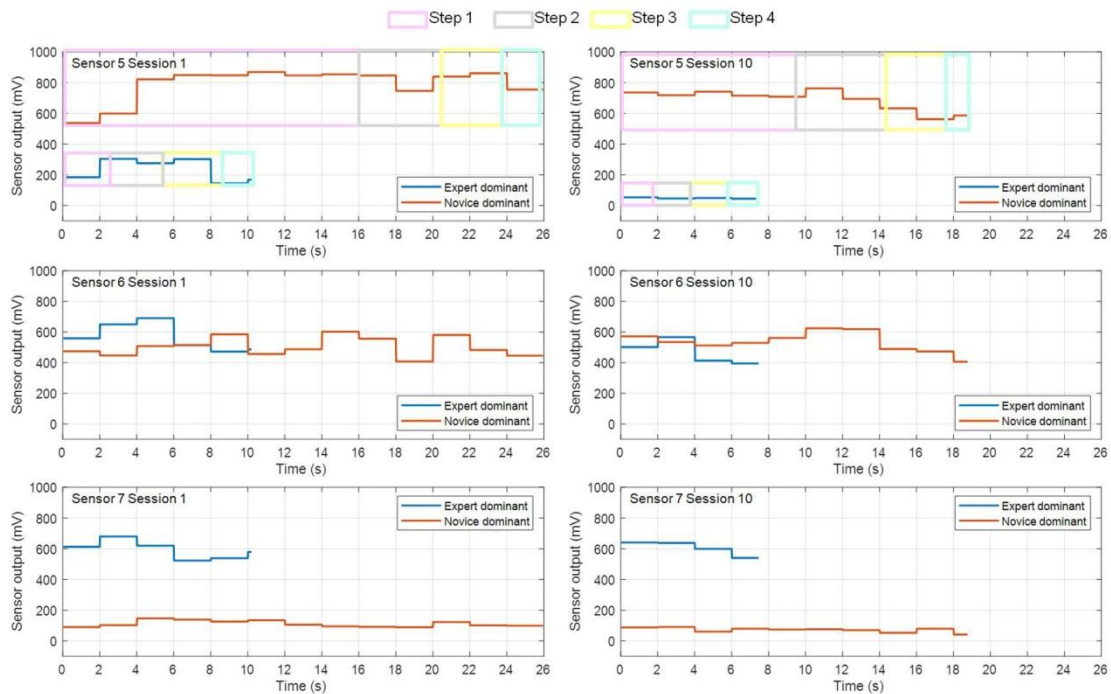


Figure 2. Individual grip force profiles showing average peak amplitudes (mV) from sensors 5, 6, and 7 for fixed successive temporal windows of 2000 milliseconds in a given session, for the first and last of ten sessions of the expert and the novice. Relative durations of each of the four critical task steps within a given session are highlighted by the colored squares.

Statistical comparison (2-Way ANOVA) between the original raw data of expert and novice from their first and last task sessions reveal significant interactions between the ‘expertise’ (2 levels) and ‘session’ (2 levels) factors for all three sensors considered here (**S5**, **S6**, **S7**). For sensor **S5** on the middle finger (gross grip force deployment), the mean (m) grip forces and their standard errors (sem) from the first session yield $m=241mV /sem=4.3$ for the expert and $m=790mV/sem=2.7$ for the novice, showing that the latter deploys about three times as much unnecessary gross grip force by comparison with the expert. This expertise-specific difference in proportional gross grip force deployed by the middle finger is even larger in the last session, with $m=78mV/sem=4.9$ for the expert, and $m=640mV/sem=3.6$ for the novice. The interaction between the ‘expertise’ and ‘session’ factors for sensor **S5** is significant with $F(1,2880)=28.65$; $p<.001$. For sensor **S6** on the ring finger (no meaningful role in grip force control), the differences between the grip force profiles of novice and expert are minimal, as would be expected, in the first session with $m=576mV /sem=3.8$ for the expert and $m=504mV/sem=2.4$ for the novice, and in the last session with $m=474mV /sem=4.5$ for the expert and $m=445mV/sem=3.3$ for the novice. The interaction between the ‘expertise’ and ‘session’ factors for sensor **S6** is, however, significant with $F(1,2880)=35.86$; $p<.001$, which is explained by the fact that grip forces, i.e. amplitudes in mV , diminish in both users from the first to the last

session, but not by the same amounts. For sensor **S7** on the small finger (critically important for fine grip force control), the expertise-specific difference between the two user profiles is characterized by the novice deploying largely insufficient grip forces, from the first session with $m=98mV/sem=1.2$ to the last with $m=78mV/sem=1.6$, while the expert produces sufficient grip force for fine movement control from the first session with $m=594mV/sem=1.8$ to the last with $m=609mV/sem=2.2$. The interaction between the ‘expertise’ and ‘session’ factors for sensor **S7** is highly significant with $F(1,2880)=188.53$; $p<.001$. Task times are considerably shorter in the expert (Figure 2), with 10.4 sec in the first session and 7.6 sec in the last indicating a minor practice effect. The novice takes more than twice as long (26 sec) in the first session compared with the expert, with a 30% time gain in the last session (18.8 sec), indicating a temporal training effect. Concerning incidents (trajectory adjustments, grip failures, drop misses), the task videos reveal a total number of 20 in the novice, and only three small trajectory adjustments in the expert’s performance.

4. Discussion

The data reveal expertise-specific differences in the spatio-temporal grip force profiles of an expert and a novice repeatedly performing a 2D image-guided robot-assisted precision task. These differences can be functionally assessed under the light of previous work [3-6] on the role of finger grip forces and prehensile synergies, centrally controlled in the human brain for optimizing human motor performance and control. One major difference as a function of task expertise or skill concerns proportional gross grip force deployed by the middle finger, with the novice deploying way too much unnecessary, task-irrelevant gross grip force, while the expert has learnt to skillfully minimize those. Another functionally important, expertise-specific difference concerns precision grip force control by the small finger, critically important in surgical and other precision tasks. Here, the difference between the two users is characterized by the novice deploying insufficient grip forces, with no major evolution between the first and the last task sessions. Concerning grip forces deployed by the ring finger, which plays no major or meaningful role in grip force control, differences between grip force profiles of novice and expert are, indeed and as would be expected, minimal and do not change much across sessions although total grip force magnitudes (mV amplitude) diminishes across sessions in both users. At the beginning, the novice takes more than twice as long performing the precision task by comparison with the expert, but at the end scores a 30% time gain indicating a considerable temporal training effect, especially in the first critical task step, as indicated by the pink boxes in Figure 2. This is readily explained by the fact that the first task step is the most difficult for a novice. It consists of moving the tool along a virtual trajectory towards the object location, and requires movement away from the body in the surgeon’s peri-personal space. This implies the perceptual recovery of physically missing depth information along a virtual z-axis in the 2D image plane. Such difficulty results in longer task times and imprecise tool-movements [7,8,9,10], explaining why the largest training gain in total task time of the novice is observed for task step 1. Finally, the analyses shown here can be run in real-time to monitor manual/bimanual precision tasks, control performance quality, or to prevent risks in robot assisted surgery for systems where excessive grip forces can cause tissue damage [11], which does not apply to this system here. The human hand has evolved as a function of active constraints in harmony with other sensory systems [12,13]. Grip force profiles are a direct reflection of the complex cognitive and behavioral synergies this evolution has produced.

Author Contributions: Conceptualization, B.D.L., R.L., F.N., P.Z and M.d.M.; methodology, R.L. B.D.L., F.N., P.Z., M.d.M.; software, F.N., R.L., P.Z., formal analysis, R.L., B.D.L., F.N.; investigation, R.L.; resources, F.N., P.Z.; data curation, R.L.; writing—original draft preparation, B.D.L., R.L.; writing—review and editing, R.L., F.N., P.Z., M.d.M, and B.D.L.; visualization, R.L.; funding acquisition, B.D.L., F.N., M.d.M.; all authors have read and agreed to the published version of the manuscript.

Funding: This ongoing work is part of a project funded by the University of Strasbourg’s *Initiative D’EXcellence (IDEX)*.

Acknowledgments: Material support by CNRS is gratefully acknowledged.

Conflicts of Interest: The authors declare no conflict of interest.

References

1. A Batmaz, AU, Falek, AM Zorn, L, Nageotte, F, Zanne, P, de Mathelin, M, Dresp-Langley, B. Novice and expert behavior while using a robot controlled surgery system In Proceedings of the 2017 13th IASTED International Conference on Biomedical Engineering (*BioMed2017*), Innsbruck, Austria, 21 February **2017**; pp. 94–99.
2. de Mathelin M, Nageotte F, Zanne P, Dresp-Langley B. Sensors for Expert Grip Force Profiling: Towards Benchmarking Manual Control of a Robotic Device for Surgical Tool Movements. *Sensors (Basel)*, **2019**;19(20).
3. VM. Zatsiorsky, ML. Latash, Multifinger prehension: an overview. *J Mot Behav*, Vol. 40, Issue 5, **2008**; pp. 446-76.
4. H. Kinoshita, T. Murase, T. Bandou, Grip posture and forces during holding cylindrical objects with circular grips. *Ergonomics*, Vol. 39, Issue 9, **1996**; pp. 1163-76.
5. H. Kinoshita, S. Kawai, K. Ikuta, Contributions and co-ordination of individual fingers in multiple finger prehension. *Ergonomics*, Vol. 38, Issue 6, **1995**; pp. 1212-30.
6. ML. Latash, VM. Zatsiorsky. Multi-finger prehension: control of a redundant mechanical system. *Adv Exp Med Biol*, Vol. 629, **2009**; pp. 597-618.
7. Batmaz, A. U., de Mathelin, M., & Dresp-Langley, B. Getting nowhere fast: Trade-off between speed and precision in training to execute image-guided hand-tool movements. *BMC Psychology*, **2016**; 4, 1535.
8. Batmaz, A.U.; de Mathelin, M.; Dresp-Langley, B. Seeing virtual while acting real: Visual display and strategy effects on the time and precision of eye-hand coordination. *PLoS ONE*, **2017**; 12:e0183789.
9. Batmaz, A. U., de Mathelin, M., & Dresp-Langley, B. Effects of 2D and 3D image views on hand movement trajectories in the surgeon’s peri-personal space in a computer controlled simulator environment. *Cogent Medicine*, **2018**; 5(1), 1426232.
10. Dresp-Langley, B. Towards Expert-Based Speed–Precision Control in Early Simulator Training for Novice Surgeons. *Information*, **2018**; 9(12):316.
11. Abiri A, Pensa J, Tao A, Ma J, Juo YY, Askari SJ, Bisley J, Rosen J, Dutson EP, Grundfest WS. Multi-Modal Haptic Feedback for Grip Force Reduction in Robotic Surgery. *Scientific Reports*, **2019**;9(1):5016.
12. Johansson RS, Cole KJ. Sensory-motor coordination during grasping and manipulative actions. *Curr Opin Neurobiol*, **1992**; 2: 815–823.
13. Dresp-Langley B, Monfouga M. Combining Visual Contrast Information with Sound Can Produce Faster Decisions. *Information*, **2019**; 10(11):346-346.

Additional material

Figure 2 large version:

